Solution Structure of a Trisaccharide–Antibody Complex: Comparison of NMR Measurements with a Crystal Structure

David R. Bundle,* Herbert Baumann,‡ Jean-Robert Brisson, Stéphane M. Gagné,§ Alexander Zdanov, and Miroslaw Cygler

Institute for Biological Sciences, National Research Council of Canada, Ottawa, Ontario, Canada K1A 0R6, and Biotechnology Research Institute, National Research Council of Canada, Montréal, Québec, Canada H4P 2R2

Received September 29, 1993; Revised Manuscript Received January 25, 1994®

ABSTRACT: NMR and crystallography have been used to study antigen conformational changes that occur in a trisaccharide–Fab complex in solution and in the solid state. NOE buildup rates from transferred NOE experiments show that the antigenic determinant of a *Salmonella* lipopolysaccharide, represented by the trisaccharide methyl glycoside α-D-Gal*p*(1→2)[α-D-Abe*p*(1→3)]-α-D-Man*p*1→OMe (**1**), undergoes a protein-induced conformational shift about the Gal→Man glycosidic linkage when it is bound by a monoclonal antibody in aqueous solution. The same trisaccharide was crystallized with Fab, and a solved structure at 2.1-Å resolution revealed that the conformation of the trisaccharide ligand was similar to that seen in a dodesaccharide–Fab complex [Cygler *et al.* (1991) *Science 253,* 442–445), where the Gal-Man linkage also experienced a similar conformational shift. Distance constraints derived from the TRNOE buildup curves are consistent with two bound trisaccharide conformations, one of which correlates with the ligand conformation of the crystalline Fab–trisaccharide complex. In this bound conformation, short interatomic distances between Abe O-2 and Gal O-2 permit an oligosaccharide intramolecular hydrogen bond. Despite its relatively low energy, a preponderance of this conformer could not be detected in aqueous or DMSO solutions of free trisaccharide by either ^{1}H or ^{13}C NMR experiments. In DMSO, a different intramolecular hydrogen bond between Abe O-2 and Man O-4 was observed due to a solvent-induced shift in the conformational equilibria (relative to aqueous solution). Molecular modeling of the trisaccharide in the binding site and as the free ligand suggested that the protein imposes an induced fit on the antigen, primarily resulting in a shift of the Gal-Man ϕ torsional angle. This reduces the interproton separation between Abe H-3 and Gal H-1 with a marked increase in the intensity of the previously weak NOEs between the protons of the noncovalently linked galactose and abequose residues. The impact of the conformational shift on gross trisaccharide topology is sufficiently small that binding modes inferred from functional group replacements are not impaired.

The preceding manuscript has described the structural requirements and binding thermodynamics of an oligosaccharide–antibody complex (Bundle *et al.*, 1994). Interpretation of this solution thermodynamic data is predicated upon an assumption that modified oligosaccharides adopt bound conformations similar to that of the bound native epitope and that the bound conformation is not far removed from the major solution conformations. Under these conditions, observed free-energy changes for functional group replacements represent incremental contributions to carbohydrate–protein interactions. However, it is increasingly appreciated that induced conformational changes often accompany ligand binding (Glaudemans *et al.*, 1990; Jorgensen, 1991; Scherf *et al.*, 1992; Stevens *et al.*, 1993). These may take the form of ligand conformational shifts (Glaudemans *et al.*, 1990; Scherf *et al.*, 1992) or shifts in antibody hypervariable loop structure (Rini *et al.*, 1992). NMR provides a convenient tool in the TRNOE[1] experiment to observe the bound ligand conformation (Clore & Gronenborn, 1982, 1983), and it has been successfully applied to antibody interactions with saccharide (Glaudemans *et al.*, 1990), peptide (Scherf *et al.*, 1992), and aromatic ligands (Bruderer *et al.*, 1992) and to lectin–saccharide interactions (Bevilacqua *et al.*, 1990, 1992). Antigen–antibody adaptations have been observed in several crystal structures (Colman, 1988; Davies *et al.*, 1990), and since oligosaccharides are to a certain extent flexible molecules, their conformation in the bound state is of particular interest.

In the previously determined crystal structure, the dodecasaccharide antigen used to obtain crystals of a Fab–antigen complex consisted of three tetrasaccharide repeating units, [→3)α-D-Gal*p*(1→2)[α-D-Abe*p*(1→3)]-α-D-Man*p*(1→4)α-L-Rha*p*(1–]$_3$. Only three sugars of one of these units were well ordered in the crystal. Because of the lack of interpretable electron density beyond this epitope, it was not possible to determine which of the three units, central or terminal, was bound in the center of the Fab variable domain (Cygler *et al.*, 1991). The principal van der Waals contacts of this epitope could be identified and a hydrogen-bonding scheme deduced. The protein–sugar recognition is dominated by the 3,6-dideoxy-α-D-*xylo*-hexopyranose residue abequose, which is totally

* Address for correspondence: Department of Chemistry, University of Alberta, Edmonton, Alberta, Canada T6G 2G2. Telephone: (403) 492-4964. Fax: (403) 492-8231.
‡ NRCC Research Associate, 1989–1991.
§ NRCC Summer Student, 1991.
® Abstract published in *Advance ACS Abstracts,* April 1, 1994.

[1] Abbreviations: Abe, abequose, 3,6-dideoxy-D-*xylo*-hexose; NOE, nuclear Overhauser effect; TRNOE, transferred NOE; HSEA, program implementing hard sphere *exo*-anomeric force field for saccharide conformation; GESA, geometry of saccharides program that implements conjugate gradient search with the HSEA force field; QCPE, quantum chemical program exchange; V_L, variable domain of immunoglobulin light chain; V_H, variable domain of immunoglobulin heavy chain; Fab, *ca.* 50 000-kDa antigen-binding fragment composed of V_L, C_L, and V_H CH1 domains and released from IgA by papain proteolysis; Fv, *ca.* 25 000-kDa antigen-binding fragment composed of V_L and V_H domains.

0006-2960/94/0433-5183$04.50/0 Published 1994 by the American Chemical Society

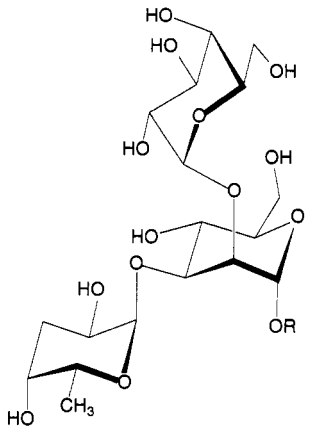

1 $R = CH_3$

2 $R = (CH_2)_8CO_2CH_3$

FIGURE 1: Structure of the trisaccharide ligand **1**.

buried in a deep pocket forming the base of the antibody-binding site. Mannose and galactose, the other two well-ordered sugars, lie on the surface of the antibody and are partially exposed to bulk water. Thermodynamic data for structural analogues (Bundle *et al.*, 1994) showed that the binding cavity is filled by the trisaccharide determinant (Figure 1), a size close to previous estimates of the minimum for anti-carbohydrate sites (Kabat, 1966).

The binding site is dominated by aromatic amino acids, and one-third of the free energy of binding, ΔG = 30.5 kJ mol^{-1}, derives from favorable entropy contributions. The thermodynamics of trisaccharide **1** binding measured over the range 10–35 °C suggested that the release of water from the binding site and nonpolar interactions make important contributions to binding (Sigurskjold & Bundle, 1992). The association constant of 2.05×10^5 M^{-1} remains constant for larger, oligomeric haptens (Sigurskjold *et al.*, 1991), and its magnitude is typical of carbohydrate–antibody interactions, even placing toward the high end of values observed for oligosaccharide epitopes. Nevertheless, association constants in this range are certainly low when compared to antibodies that bind proteins (Lavoie *et al.*, 1992) or ligands such as fluorescein (Herman *et al.*, 1989).

To date, only one crystal structure of an antibody (Se155-4) complexed with oligosaccharide has been reported (Cygler *et al.*, 1991), although a solved crystal structure of a similar complex is at the refinement stage (Vyas *et al.*, 1993). Consequently the Se155-4 system provides a unique opportunity to compare the oligosaccharide–Fab crystal structure with the corresponding solution structure, at least for the bound ligand. The crystal structure of saccharide-free, native Fab indicates only small amino acid side chain movements when the carbohydrate ligand is bound, which raises the possibility that the trisaccharide intramolecular hydrogen bond observed in the crystal structure corresponds to a significantly populated solution conformer. Besides shedding light on the specific details of this binding site, investigation of these possibilities is generally relevant to attempts to understand the relationship of oligosaccharide solution conformations to those of the bound state and whether there are experimental grounds to model the solution conformation of oligosaccharides with explicit terms to describe intramolecular hydrogen-bond formation in solution (Cumming & Carver, 1987; Poppe *et al.*, 1992). One example of pronounced oligosaccharide conformational change on binding to antibody has been reported (Glaudemans *et al.*, 1990), while lactose binding to ricin shows only small shifts in the glycosidic torsional angles (Bevilacqua *et al.*, 1990). It has also been demonstrated that antibodies impose on bound peptides conformations that are either not populated at all or significantly different from those sampled in aqueous solution (Scherf *et al.*, 1992). Evidence has also been presented for antibody-induced conformational changes of DNA ligands (Stevens *et al.*, 1993).

Here, we investigate the conformation of the trisaccharide Gal[Abe]Man (**1**) in solution and in a complex with the Fab fragment and compare it to the previously studied properties of the free antigen (Bock *et al.*, 1984a,b). Since the location of the trisaccharide epitope within the trimeric dodecasaccharide as observed in the published crystal structure is uncertain (Cygler *et al.*, 1991), the conformation of this epitope could be affected by the disordered parts. To have a good reference point for comparison with solution studies, we have crystallized the complex of the Se155-4 Fab fragment with the isolated trisaccharide epitope as its methyl glucoside **1** and determined its three-dimensional structure. Model complexes such as these may be relevant to the heighten interest in the potential of carbohydrate-based drugs, where general approaches toward the observation of bound ligand conformation and its modeling with protein receptors are needed.

EXPERIMENTAL SECTION

Materials. Trisaccharide **1** was available from chemical synthesis (Bundle & Eichler, 1994). Antibody Fab was prepared in proteolysis and affinity purification according to the procedure described in the accompanying paper (Bundle *et al.*, 1994).

Crystallization and Data Collection. The crystals of Fab–trisaccharide complex were grown by the vapor-diffusion method under conditions similar to those previously described (Rose *et al.*, 1990). Fab fragment in 10 mM Tris-HCl buffer, pH 8.0, and 0.1 M NaCl was concentrated to 7.3 mg/mL. Trisaccharide was dissolved in distilled water to a concentration of 10 mg/mL. The well solution contained 15% polyethyleneglycol 8000 and 50 mM Tris-HCl buffer, pH 7.5, and drops were prepared by mixing 3 μL of Fab and 4 μL of well solution with 1 μL of trisaccharide. After preequilibration, nucleation was induced by microseeding with crushed crystals of uncomplexed Fab. Large crystals suitable for data collection were obtained by repeated macroseeding. They belong to the $P2_12_12_1$ space group with cell dimensions a = 47.3, b = 129.3, and c = 79.9 Å.

X-ray diffraction data were collected on a R-AXIS II image plate area detector installed on a Rigaku RU-300 rotating anode generator. Ninety frames with oscillation of $\Delta\varphi$ = 1.5° and 30-min exposure time were collected and processed. A total of 86 916 observations with $I > \sigma(I)$ were reduced to 24 335 independent reflections with R_{sym} = 4.7%. The completeness of data to 2.1-Å resolution is 81%.

Structure Determination and Refinement. The crystals of the trisaccharide complex are isomorphous to the previously determined dodecasaccharide–Fab structure (Cygler *et al.*, 1991). The coordinates of only the Fab fragment from the previous complex were refined against the new data. Rigid-body refinement with the program X-PLOR (Brunger, 1993) was followed by conjugated gradient minimization and model refitting. The trisaccharide was then built into the difference electron density map. Further refinement included an additional 95 water molecules and resulted in the R factor 0.183 for data in the 8–2.1-Å resolution range and with $I > 2\sigma(I)$. The root-mean-square deviations of bond lengths and

bond angles from the standard values are 0.013 Å and 3.1°, respectively.

Instrumental Methods. ^1H and ^{13}C NMR spectra were recorded on a Bruker AMX 600 NMR spectrometer. Experiments were performed without sample spinning and used standard software provided by Bruker.

Protein NMR Sample Preparation. Fab (*ca.* 10 mg) dissolved in PBS, pH 7.0, was concentrated to approximately 1 mL by ultrafiltration in Centricon concentrators (Amicon), lyophilized twice with D_2O, and dissolved in D_2O (650 μL). Aliquots (20 μL) were diluted to 1 mL for determination of protein concentration by UV absorbance at 280 nm. Solutions of 0.17 mM Fab used for NMR experiments contained 4.9 mg of protein in 550 μL of PBS in D_2O, pD 7.2.

Resonance Assignment. Unambiguous resonance assignment for trisaccharide **1** in D_2O and DMSO-d_6 solutions was accomplished via homonuclear and heteronuclear correlation spectroscopy.

Detection of Intramolecular Hydrogen Bonds. (A) DMSO Solution. A 20 mM solution of trisaccharide **1** in DMSO-d_6 (99.99%, 0.5 mL) was titrated with 0.5-μL aliquots of D_2O until 75% of hydroxyl protons were deuterated. After each addition, a ^1H NMR spectrum was acquired at 27 °C, FIDS were zero-filled to give a final digital resolution of 0.1 Hz/point, and a Gaussian function was applied prior to Fourier transformation.

(B) H_2O Solution: ^1H Detection. A sample of **1** dissolved in D_2O and eluted from Chelex resin was dried and dissolved in 85% H_2O:15% acetone-d_6 to give a 100 mM solution. ^1H NMR spectra were recorded at temperatures from 27 to −14 °C. Water suppression was accomplished with a 1–1 echo sequence (Sklenar & Bax, 1987).

(C) H_2O solution: ^{13}C Detection. Chelex-treated **1** was dissolved in a H_2O:D_2O mixture (1:1 v/v), and ^{13}C NMR spectra were recorded for a 40 mM solution at various temperatures in the range −7–40 °C.

T_1 Measurements. ^1H and ^{13}C relaxation measurements (Table 4) were performed at 37 °C by the inversion-recovery technique (Freeman & Hill, 1971) using standard Bruker pulse programs and software to calculate T_1 values.

Steady-State NOE Measurements. Difference NOE spectra were recorded for 20 mM trisaccharide solution in D_2O at 37 °C. Multiple irradiation was employed for multiplets (Neuhaus, 1983; Kinns & Saunders, 1984), and with a total irradiation time of 1 s and a 5-s relaxation delay, the recycle time was 6.5 s.

TRNOE Measurements. All measurements were performed at 37 °C. Trisaccharide **1** (15 molar equiv) dissolved in 30 μL D_2O was added in 2-μL aliquots to a 550-μL Fab solution in a 5-mm NMR tube to a final concentration of 0.17 mM Fab and 2.55 mM trisaccharide. Line broadening of the *O*-methyl resonance was checked after each addition of ligand, and a one-dimensional NOE difference spectrum was recorded for 5, 10, and 15 molar equiv of **1**. At 37 °C and a ligand:Fab ratio of 15:1, the transferred NOE appeared to be optimal and two-dimensional NOESY experiments were recorded at various mixing times. The relaxation times for saccharide ring protons in the sample used for TRNOE did not differ substantially from those measured for the free ligand (Table 4).

Phase-sensitive NOESY using TPPI and presaturation of the HDO signal were recorded for mixing times of 50, 75, 100, 150, 200, 250, and 300 ms. The temperature was maintained at 37 °C for the duration of the experiments, and 48 scans were collected per t_1 increment with a pulse delay of 2.5 s for a minimum recycle time of 3 s. The sweep width was 7300 Hz in both dimensions, and the initial (t_1, t_2) matrix of 512 × 4096 data points was zero-filled to give a digital resolution of 7.2 and 3.6 Hz/point, respectively. A $\pi/2$-shifted squared sine bell filter was applied to both dimensions prior to Fourier transformation. The base line was corrected in f_2 (first order polynomial) prior to integration of cross-peak volumes.

Potential Energy Calculations. Rigid-body potential energy calculations were performed for the trisaccharide 3-*O*-methyl-α-D-Gal*p*(1→2)-[α-D-Abe*p*(1→3)]-α-D-Man*p*1→OMe using the program GESA (Meyer, 1990) that is based upon the HSEA force field (Thøgersen *et al.*, 1982). Monosaccharide coordinates were generated from X-ray coordinates minimized with MM3(87) (QCPE) (Burket & Allinger, 1982). The ϕ,ψ energy maps were calculated for each glycosidic linkage at 5° intervals. For a given linkage, the map was obtained by choosing the minimum energy for each point (rigid-body relaxed map). As an option in HSEA calculations, a hydrogen-bond potential could be applied (Perez *et al.*, 1984). Similarly, the linkage maps were calculated using the CHARMm potential modified for carbohydrates (see below).

Ensemble-Averaged NOE. Interatomic proton distances used to calculate ensemble-averaged NOE values were calculated by the GESA program as previously reported (Peters *et al.*, 1990) and expressed as $\langle r^{-3}\rangle^{-2}$ prior to weighting according to the Boltzman distribution function. A motional correlation time, of $\tau_c = 0.25$ ns was selected from the fit of calculated and observed NOE for the known distance Gal H-1 to Gal H-2 within a single hexose residue. Potential errors that may arise due to this simplified approach include anisotropic reorientation and internal motions about the glycosidic linkage that may exist on a time scale approaching that of overall tumbling (Hricovini *et al.*, 1992).

CHARMm Force Minimization of the Trisaccharide Fv Complex. Energy minimizations were done using the molecular dynamics program CHARMm (Brooks *et al.*, 1983). The parameter set for carbohydrates was based on the approach used by Homans (Homans, 1990) which combines literature monosaccharide parameters (Ha *et al.*, 1988) and includes an additional energy term to take account of the *exo*-anomeric effect for the glycosidic linkages (Wiberg *et al.*, 1989). Using Quanta (Molecular Simulations), monosaccharide units were constructed employing the starting X-ray coordinates, minimized with CHARMm. The trisaccharide was assembled with the Gal and Man residues methylated at the site of glycosidic linkages in the polysaccharide. The Fv coordinates were obtained from the crystal structure.

Energy-Minimized Complex. Energy minimizations on the protein–carbohydrate complex were performed using 1000 steps of conjugate gradient minimization. The nonbonded pair list was updated every 50 iterations, and a cutoff of 8 Å was used. A distance-dependent dielectric constant was also used. No hydrogen-bonding potential was utilized. The trisaccharide starting structure and the water molecule in the binding site were oriented as in the X-ray structure of the complex (Cygler *et al.*, 1991). When the minimum-energy conformer of **1** was modeled into the binding site, it was initially positioned to overlay the abequose coordinates of the solved complex.

Bound Conformation by NMR. TRNOE distance constraints were imposed, while ϕ,ψ torsion angles were varied for both linkages and torsional angles which satisfied two distance constraints were kept. The potential energy was calculated for all these conformers, with and without a

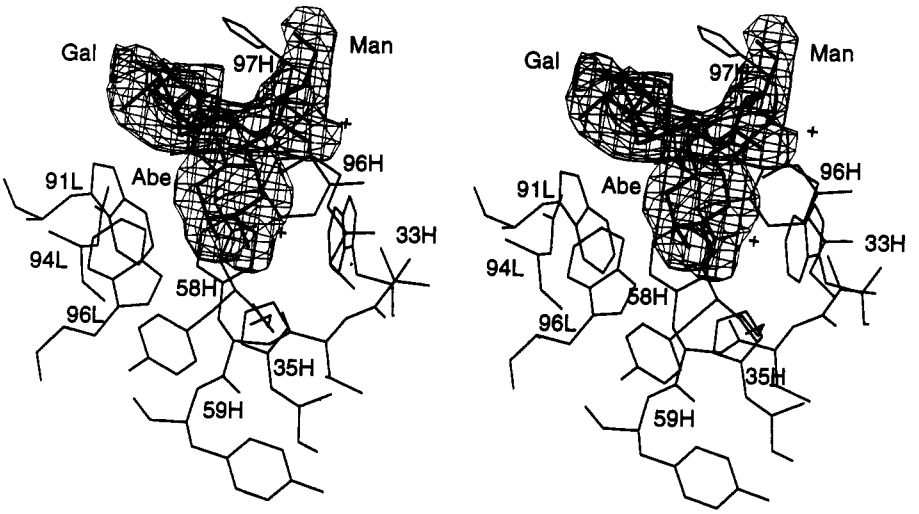

FIGURE 2: Stereo plot of the electron density describing the trisaccharide conformation in the binding site.

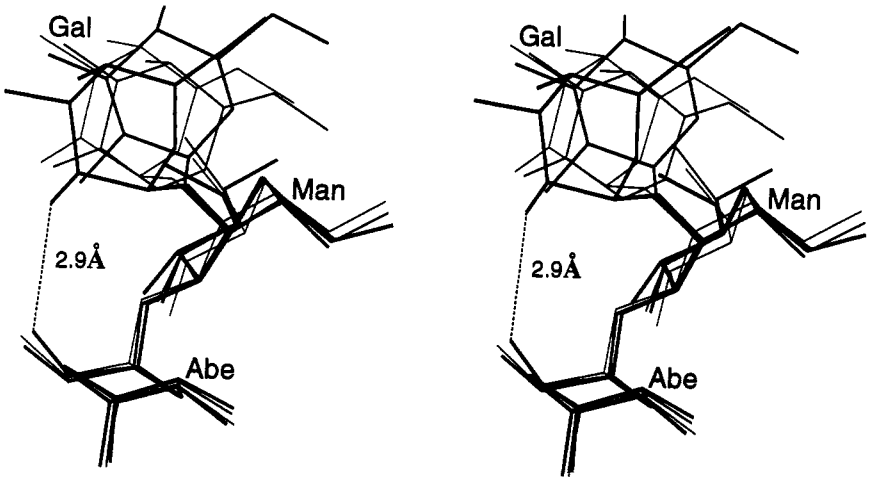

FIGURE 3: Relative orientation of the galactose residue in the different conformations of trisaccharide **1**. In order of decreasing thickness: bound conformer by crystallography, minimum-energy conformer, conformers determined by TRNOE experiments.

hydrogen-bonding potential (Perez *et al.*, 1984), and the lowest energy minima were selected.

RESULTS AND DISCUSSION

Bound Trisaccharide Conformation in the Crystal. To minimize a bias in the comparison of the NMR and crystallographic results, the crystal structure of a Fab–trisaccharide complex has been determined, rather than relying upon inferences drawn from the solved structure of the dodecasaccharide–Fab complex (Cygler *et al.*, 1991). All three hexose residues of the trisaccharide are clearly defined in the electron density map (Figure 2), and the trisaccharide binds in the same position and in a similar conformation (Figure 3) to that observed in the Fab–dodecasaccharide complex (Cygler *et al.*, 1991). The abequose occupies a deep pocket near the pseudo-2-fold axis of the variable domain, while the two other sugars extend along the protein surface in a direction nearly perpendicular to the V_L/V_H interface. The hydrogen-bond interactions of Abe with Fab are mediated by a water molecule bound tightly at the bottom of the pocket (preceding manuscript, Figure 9). The conformation of the Man-Gal linkage is the same as in the previous complex where the hydroxyls of Abe O-2 and Gal O-2 are within hydrogen-bonding distance (Table 1). An additional water molecule (wat2) bridges between the antigen, Man O-4, and Fab (Trp 33H). Most likely, Man O-4 which accepts a hydrogen bond from His 97H also donates its hydroxyl proton to this bound water molecule (Table 1). The hydrophobic interactions are identical to those observed in the dodecasaccharide complex (Cygler *et al.*, 1991). The similarity of the conformations of the trisaccharide epitope in the two complexes may indicate that it is the repeating unit from the nonreducing end of the dodecasaccharide that is uniquely bound to the Fab fragment in the previously published crystal structure.

Table 1: Hydrogen-Bond Contacts and Contact Surface Area between the Oligosaccharide and Fab Fragment and Ordered Water Molecules

antigen atom	distance (Å)	bridging atom	distance (Å)	contacting atom
Abe				
O-2			2.7	N(Gly98H)
O-2			3.0	O-2(Gal)
O-4			2.9	NE1(Trp96L)
O-4	2.8	O(wat1)	2.9	NE2(His35H)
O-5	3.0	O(wat1)	2.9	O(Gly96H)
		O(wat1)	3.0	O(Tyr99H)
Man				
O-4			2.9	Nδ1(His97H)
O-4	2.7	O(wat2)	3.0	Nε1(Trp33H)
Gal				
O-2			2.9	O-2(Abe)
O-4			3.3	Nε1(Trp91L)
O-3			3.7	Nε2(His32L)

Energy Minimization of the Trisaccharide by HSEA and CHARMm Force Fields. Potential energy maps for each of

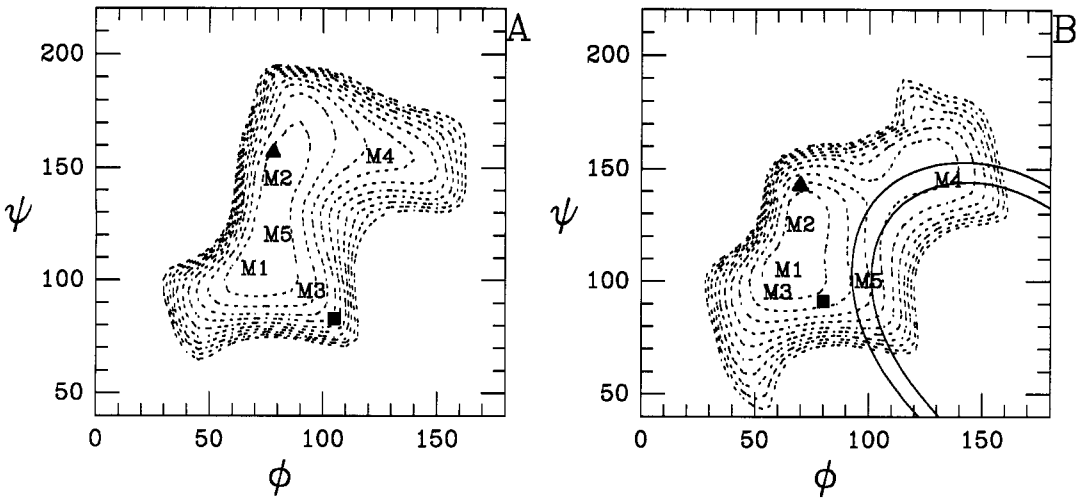

FIGURE 4: Potential energy map for the *Salmonella* trisaccharide for the Gal(1→2)Man linkage (A) and the Abe(1→3)Man linkage (B). With respect to the global minimum of each map, 4 kJ mol^{-1} energy levels up to 40 kJ mol^{-1} are drawn. In (B), the band, which encompasses M4 and M5, is for the (Abe O-2, Man O-4) hydrogen-bond distance within 2.8–3.1 Å. The glycosidic torsional angles of the bound conformer determined by crystallography are indicated by ■ and those of the CHARMm minimum by ▲.

the glycosidic linkages were calculated using different variants of the HSEA force field without and with a hydrogen-bonding term. The rigid-body approach (HSEA) gave distinct, characteristically steep global energy minima, and for each glycosidic linkage, the potential energy maps show the position of the global minimum, M1, and the subsequent local minima, M2–M5 (Figure 4). The conformation of the glycosidic linkage in the bound state as determined by crystallography is also marked on the ϕ,ψ maps. Vicinal branching at the 2- and 3-positions of the mannose residue imposes limitations on the flexibility of each linkage, although to a lesser extent on the Gal-Man (Figure 4A) than on the Abe-Man linkage (Figure 4B) (Bock *et al.*, 1984a). However, the conformational space defined by the 40 kJ mol^{-1} energy bounds is similar, and it is clear that both glycosidic linkages may sample a fairly broad range of torsion angles within the potential energy range 0–13 kJ mol^{-1}. While the bound conformation determined by crystallography lies within 5 kJ mol^{-1} of the global minimum for the Abe-Man linkage (Figure 4B), a significant departure in ϕ of 40° places the Gal-Man linkage 16 kJ mol^{-1} from its global minimum-energy conformation (Figure 4A).

The CHARMm force field parametrized for carbohydrates was also used to calculate linkage maps and for potential energy calculations that include simulated environments of different dielectric constant. The CHARMm global minimum was close to that calculated by the HSEA force field; however, as expected from an approach that treats explicitly valence-angle fluctuations and bond deformations, etc., the resultant minima were broader. The relative positions of the CHARMm, HSEA, and bound crystal structure conformation are displayed on the Gal-Man ϕ,ψ map (Figure 4B).

In the subsequent treatment of experimental data, the potential energy surfaces were utilized for two purposes: (i) modeling the experimentally determined NOE data for the free trisaccharide **1**, as described by Peters and co-workers (Peters *et al.*, 1990), and (ii) interpreting TRNOE-derived distance constraints for bound **1** in terms of energetically plausible conformations.

Modeling the Trisaccharide Fv Complex. Via the coordinates of the Fv including the bound water molecule at the base of the binding site, two trisaccharide conformers were positioned in the binding site and subjected to energy minimization with and without a distance-dependent function for dielectric constant. When the conformer observed in the crystal structure was used as the initiation point, there was a small deviation from the starting conformation but the bound conformation rapidly converged and remained close to that of the crystal structure. Conversely, when the HSEA minimum-energy conformer was used as the starting point, it steadily converged to the torsional angles observed in the solved crystal structure. This was the case both with and without the distance-dependent dielectric constant. When this function was applied, there were clear indications that the intramolecular hydrogen bond was formed between the Gal O-2 and Abe O-2 atoms.

Resonance Assignment. Earlier work has reported a simple conformational model for the solution NMR of 3,6-dideoxyhexose containing epitopes of *Salmonella* (Bock *et al.*, 1984a,b). For the most part, these structures were covalently attached to a C_9 linking arm (Lemieux *et al.*, 1975). The chemical shifts of trisaccharide **1** compared to those of trisaccharide **2** differed slightly, and as a prelude to the TRNOE experiments, trisaccharide **1** was subjected to rigorous assignment of ^{1}H and ^{13}C NMR chemical shifts recorded at 600 and 150 MHz (Tables 2 and 3). Assignments for solutions in D_2O and DMSO-d_6 (Figure 2A) were based on COSY, TOCSY, and HMQC experiments. Since exchangeable protons are observed in dry DMSO solution, these resonances were also assigned. At 37 °C in DMSO, the OH resonances overlapped, but at 17 °C, they were resolved and, in turn, assigned via a COSY experiment (Table 2).

Intramolecular Hydrogen Bonds. The crystal structure of the trisaccharide–Fab complex shows an Abe O-2 to Gal O-2 interatomic distance of 3.0 Å (Table 1). If this hydrogen bond is present in trisaccharide conformers that are populated in aqueous solution, it should be detectable by NMR methods such as those recently applied to sucrose and sialyl lactose (Poppe & van Halbeek, 1991, 1992; Poppe *et al.*, 1992). Generally, it has been difficult to observe intramolecular hydrogen bonds in aqueous solutions due to chemical exchange phenomena, but pre-steady-state NOE experiments (Poppe & van Halbeek, 1991) and isotope effects of O^1H/O^2H hydroxyl groups on ^{13}C NMR chemical shifts (Chistofides *et al.*, 1986) may be used to detect intramolecular hydrogen bonds for oligosaccharides dissolved in H_2O solutions (Poppe *et al.*, 1992). Both methods were employed here, together with the use of DMSO-d_6 as solvent to minimize the chemical

Table 2: ^{1}H NMR Chemical Shifts for Trisaccharide **1** in DMSO-d_6 at 17 °C and in D_2O at 37 °C

residue	solvent	1	2	3ax	3eq	4	5	6	6′	OMe
mannose	D_2O	5.065	3.976	3.97[a]		3.950	3.652	3.786	3.903	3.415
	DMSO	4.802	3.675	3.67[a]		3.670	3.314	3.454	3.662	3.260
hydroxyl groups						4.898		4.548		
galactose	H_2O	5.143	3.782	3.905		3.992	4.062	3.738[b]	3.738[b]	
	DMSO	4.840	3.551	3.496		3.682	3.735	3.454[b]	3.454[b]	
hydroxyl groups			3.782	4.663		4.427		4.595		
abequose	H_2O	5.098	4.022	1.976[b]	1.976[b]	3.864	4.098	1.180		
	DMSO	4.828	3.766	1.786	1.685	3.496	3.929	0.995		
hydroxyl groups			4.279			4.563				

[a] Values obtained from H/C-correlated HMQC spectrum. [b] Strongly coupled.

Table 3: ^{13}C NMR Chemical Shifts for Trisaccharide **1** in DMSO-d_6 and D_2O at 27 °C

residue	solvent	1	2	3	4	5	6	OMe
mannose	D_2O	99.40	78.54	78.73	66.53	73.72	60.96	54.24
	DMSO	100.19	78.82	78.44	67.37	73.42	61.61	
galactose	D_2O	101.68	68.77	69.69	69.03	71.52	60.77	
	DMSO	102.03	69.48	70.12	70.12	72.20	62.19	
abequose	D_2O	100.83	63.28	34.87	67.51	66.17	16.77	
	DMSO	101.23	64.19	33.66	69.04	67.57	16.17	

exchange of labile protons (Lemieux & Bock, 1982).

One-dimensional spectra were recorded according to published procedures using a H_2O/acetone-d_6 solvent mixture that allows the temperature to be lowered to −14 °C without freezing (Poppe *et al.*, 1991). Under these conditions, no hydroxyl protons could be observed between 27 and −3 °C. At −11 and −14 °C, only very broad OH resonances could be detected, consistent with an absence of strong or persistent hydrogen bonds.

Deuterium isotope shifts of ^{13}C resonances bearing hydroxyl groups have been observed in 1:1 H_2O:D_2O solutions. In this system, intramolecular hydrogen-bonded ^{13}CH-OH fragments appear as broadened resonances (Christofides *et al.*, 1986; Poppe *et al.*, 1992). Again, in the temperature range 27 to −7 °C, minimal line broadening was observed especially for Abe C-2 and Man C-4, which were among the sharpest signals.

A final attempt was made to observed intramolecular hydrogen bonds by dissolving the anhydrous trisaccharide in dry DMSO and observing the ^{1}H NMR spectra as increasing amounts of D_2O were titrated into the trisaccharide solution. Hydrogen-bonded OH resonances, that in the simplest case appear as doublets (Figure 5A,B), experience isotope shifts and appear as multiplets as D_2O is added (Figure 5C–E), allowing the identification of the donor and acceptor pair (Lemieux & Bock, 1982, 1984). It is clearly seen (Figure 5C–E) that a hydrogen bond is present between Abe O-2 and Man O-4 in DMSO solution. Paradoxically, in 1:1 H_2O:D_2O, the carbon atoms Abe C-2 and Man C-4 were the sharpest resonances, which is inconsistent with an Abe O-2 to Man O-4 hydrogen bond in water.

Although no hydrogen bonds could be detected in water, in DMSO a distinct hydrogen bond was evident, albeit between a different donor/acceptor pair than that observed in the crystal structure. It is concluded that in water the intramolecular saccharide–saccharide hydrogen bonds are weak and not sufficiently strong to stabilize a preferred conformation and if formed at all, they are only transient as various families of conformations are sampled. In DMSO, the conformational behavior of the trisaccharide must be different to that in water, with at least a shift in the populated conformational microstates. If an Abe O-2 to Man O-4 distance of 2.8 ± 0.25 Å is assumed for a hydrogen bond, the Abe-Man torstional angles that satisfy this condition (Figure 4A) are substantially

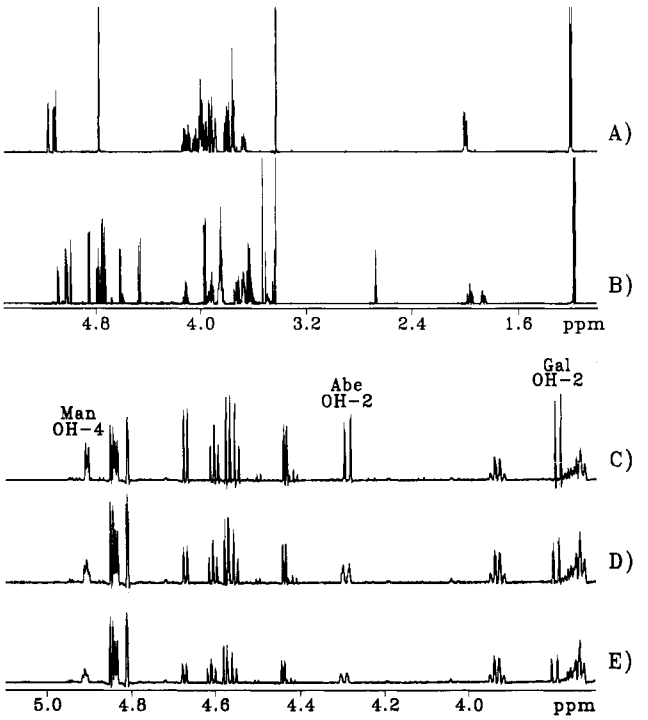

FIGURE 5: Proton NMR spectrum of **1**: (A) in D_2O at 37 °C, (B) in DMSO-d_6 at 37 °C, and (C)–(E) in DMSO-d_6 at 17 °C to which increasing amounts of D_2O have been added.

shifted from the global minimum conformation. A similar DMSO-dependent conformational shift has been reported for the galabiose structure α-D-Gal*p*(1→4)-β-D-Gal*p* (Bock *et al.*, 1988).

Relaxation and NOE Measurements for the Trisaccharide **1**. Although the principal interest of this study is the conformation of the ligand in the bound state, it is important to develop an appreciation of the solution properties of the antigen for comparison with the bound state. In order to accomplish this, NOEs and longitudinal relaxation rates were measured to obtain estimates of interproton distances (particularly those that span interglycosidic linkages) and the extent to which the overall motion of the trisaccharide departs from isotropic tumbling.

The $^3J_{H,H}$ coupling constants for **1** were similar to those reported for spectra of **2** measured at 500 MHz (Bock *et al.*, 1984b) and are consistent with the adoption by all three hexoses of stable $^4C_1$ chair conformations. ^{1}H and ^{13}C T_1 measurements (Table 4) provide general information about the overall motion of the trisaccharide and allow estimates of the time constant of reorientation, τ_c, the motional correlation time (Allerhand *et al.*, 1971) that is incorporated into the NOE simulations (Bock *et al.*, 1990). Carbon T_1 values ranging from 0.39 to 0.56 s indicate that the trisaccharide has anisotropic components to its tumbling, but if an average ^{13}C

Table 4: T_1[a] Data for Trisaccharide **1** in D_2O at 37 °C

residue		1	2	3	4	5	6	OMe
mannose	^{13}C	0.39[a]	0.45	0.44	0.45	0.47	0.56	3.83
	^{1}H	1.10				1.15		3.00
galactose	^{13}C	0.50	0.52	0.53	0.54	0.54	0.78	
	^{1}H	0.86						
abequose	^{13}C	0.54	0.51	0.56	0.56	0.52	2.07	
	^{1}H	1.09	1.63		1.10	0.79	1.90	

[a] NT_1 data, estimated error of ±0.05 s, for ^{13}C, where N is the number of directly bonded protons.

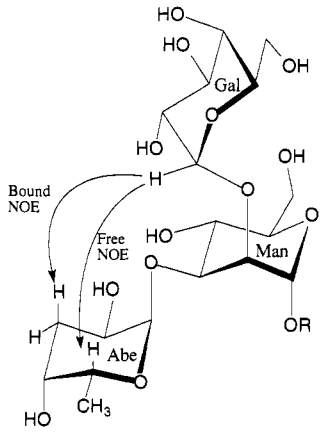

FIGURE 6: NOE connectivities between the Abe and Gal residues observed in free and bound states.

T_1 of 0.5 s for the ring carbon atoms is assumed, τ_c is estimated to be 0.11 ns. This compares to a value for τ_c of 0.25 ns estimated from the magnitude of the observed NOE values for trisaccharide **1** in D_2O. The discrepancy is consistent with anisotropic tumbling and may also indicate the existence of internal motions.

One-dimensional NOE data were determined and used to assess the conformational preference of the trisaccharide in D_2O. The observed data are similar to those previously recorded for the 8-(methoxycarbonyl)octyl trisaccharide glycoside **2** (Bock *et al.*, 1984b). Replacing this bifunctional linking arm (Lemieux *et al.*, 1975) by the methyl group increased the separation of the anomeric resonances and assisted the quantitation of the one-dimensional NOEs. Important NOEs are observed when each anomeric protons is irradiated, including intra-residue H-1 to H-2 NOEs that may be used for internal calibration of quantitative NOEs, since in a rigid $^4C_1$ chair conformation this is a known and fixed distance. Typical inter-residue NOEs are observed, Abe H-1 to Man H-3 and Gal H-1 to Man H-2, but unlike many oligosaccharides where only these single NOEs define the contacts across the glycosidic linkages, here additional inter-residue NOEs are observed, Man H-1 to Gal H-5 and Gal H-1 to Abe H-3ax and Abe H-5 (Figure 6). The latter two NOEs are crucial to the conformational change reported by the TRNOE experiment, since these NOEs relate two residues that are not covalently linked to each other. Overlap of the H-3ax and H-3eq protons required that the NOEs were calculated for simultaneous saturation of both protons. No major differences were found since the contributions from H-3eq to the NOE of H-3ax were small in all cases. Observed NOEs are compared with values calculated for the global or local minima M1–M5 or the ensemble-averaged values. These were derived assuming a Boltzman distribution of conformational microstates across the HSEA potential energy surface calculated with and without a hydrogen-bonding term.

Table 5: Comparison of Observed Relative NOE[a] with NOEs Predicted for Ensemble-Averaged Conformations and Five Distinct Conformational Minima, M1–M5

dipolar interactions		exp[b]	$\langle r^{-3}\rangle^2$	$\langle r^{-3}\rangle^2$ (HB[c])	M1	M2	M3	M4	M5
Man H-1	Man H-2	100	100	100	100	100	100	100	100
	Gal H-5	94	180	93	212	193	59	9	165
	OCH_3	116	71	69	63	84	68	66	60
Gal H-1	Gal H-2	100	100	100	100	100	100	100	100
	Man H-2	139	55	59	39	61	69	67	77
	Abe H-3	11	5	6	18	<1	20	<1	<1
	Abe H-5	41	27	23	44	43	29	<1	33
Abe H-1	Abe H-2	100	100	100	100	100	100	100	100
	Man H-3	126	80	74	68	102	46	122	126
Abe H-3	Abe H-4	100	100	100	100	100	100	100	100
	Abe H-2	46	95	95	96	96	96	92	94
	Abe H-5	46	25	26	21	21	26	37	33
	Gal H-1	14	10	13	39	1	39	<1	2

[a] Calculated NOE using a motional correlation time τ_c = 0.25 ns. [b] Estimated relative error ±20%; for NOE (<10), error ±50%. [c] With hydrogen-bonding term in potential energy.

Quantitative interpretation of the NOEs measured for **1** in D_2O in terms of single conformers or ensemble averaging showed that no single conformer nor averaged interproton distances accounted for the experimental data. Several factors contribute to this observation. Independent measurements of τ_c from ^{13}C T_1 values or from fitting the intensity of NOEs to known interproton distances reveal that motional reorientation is not isotropic and, in the light of recent work (Hricovini *et al.*, 1992), further suggest that internal motions may exist on a time scale that approaches overall tumbling. This situation places severe limitation on the quantitative treatment of NOEs as conformational constraints in assessing oligosaccharide conformation (Hricovini *et al.*, 1992). Nevertheless, it is clear from Table 5 that NOEs to be expected from any of the local minima M1–M5 are sensitive to ϕ,ψ changes and simple ensemble averaging with or without a hydrogen-bonding potential does not reproduce the observable NOEs. The anisotropic motions together with the internal motions likely represent the most significant sources of error.

This flexibility and conformational dependence on solvent may be contrasted with the rigidity reported for blood group epitopes (Lemieux *et al.*, 1980; Thøgersen *et al.*, 1982; Cagas & Bush, 1990) but is consistent with recent interpretations of oligosaccharide flexibility (Poppe & van Halbeek, 1991; Hricovini *et al.*, 1992).

Bound Trisaccharide Conformation Determined by TR-NOE. When the trisaccharide was added to Fab, one-dimensional NOE experiments showed that previously positive NOEs (Figure 7A) became negative, indicating that the experiment was sampling the bound conformer. Univalent antibody Fab fragment was used for these experiments at a final trisaccharide **1**:Fab molar ratio of 15:1. The conditions for the two-dimensional TRNOE experiment were optimized by performing one-dimensional NOE experiments at 25 and 37 °C and at trisaccharide to Fab ratios of 5, 10, and 15. Negative NOEs were observed under all conditions; however, they were optimal at 15 trisaccharide equiv and 37 °C (Figure 7B).

The off rate for the Fab–trisaccharide complex was estimated from line-broadening studies of a ^{13}C-labeled disaccharide analogue of **1** (galactose replaced by a methyl ether; compound **16** of the preceding manuscript) that binds to Fab with an affinity similar to **1** (Bundle *et al.*, manuscript in preparation). Under the conditions of temperature, ligand excess, and Fab, the off rate fell in the range 170–200 s^{-1},

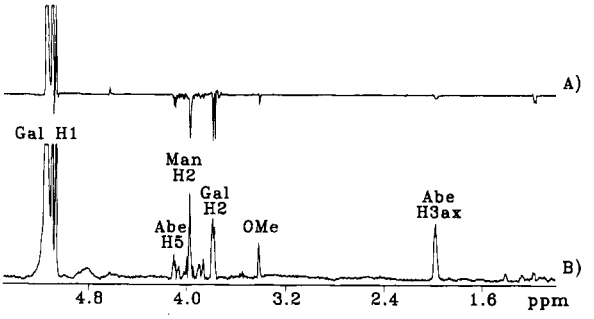

FIGURE 7: Noe experiments for the free and bound ligand. (A) One-dimensional NOE difference spectrum for the free ligand for saturation of Gal H-1, where Abe H-5 experiences a positive NOE of intermediate intensity, while the one to Abe H-3ax is weak. The Man H-1 and Abe H-1 resonances were partially saturated (<10%) and do not contribute to the observed NOEs. (B) Trace of two-dimensional NOESY experiment for the complex of Fab with **1** showing the negative NOE of the Gal H-1 resonance. In the bound state, the NOE to Abe H-3ax becomes strong while the relative NOE to Abe H-5 becomes weaker. The two signals adjacent to Gal H-1 arise from the trailing edges of the diagonal peak of Abe and Man H-1.

corresponding to fast exchange on the proton spin lattice relaxation time scale. Therefore, spin diffusion effects are not expected to be severe, and the subsequent experiments with short mixing times suggest that such relaxation pathways seen by others (Bevilacqua *et al.*, 1990, 1992) do not complicate the analysis reported here (Figure 8).

A series of phase-sensitive NOESY experiments were recorded for seven discrete mixing times in the range 50–300 ms. A typical cross-section through the projection including Gal H-1 compares the NOEs of the bound ligand with the positive NOEs observed for trisaccharide in the absence of Fab (Figure 7). The TRNOEs were quantified by integrating cross-peak volumes, and these are plotted as buildup curves (Figure 8A). It is noticeable that the seventh and last experiment (a mixing time of 250 ms) has smaller cross-peak volumes that result from lost activity of the antibody after prolonged exposure (5–7 days) to the experimental conditions. When the volumes were normalized by relating volume ratios to interproton distances (Baleja *et al.*, 1990), the NOE buildup curves were extrapolated to interproton distances at zero mixing time (Figure 8B). These distances were then compared with interproton distances seen for different conformational families predicted by modeling studies. The number of interproton distance constraints obtained from the TRNOE experiment is insufficient to define a unique bound conformation. Consequently, self-consistent solutions that satisfy the set of interproton distances were compared with energetically accessible conformers.

Conformations of trisaccharide **1** that lie within the 40 kJ mol^{-1} potential energy contour and satisfy distance constraints between the noncovalently linked Abe and Gal residues (Gal H-1/Abe H-3ax and Gal H-1/Abe H-5) in the bound state are displayed in Figure 9A–D. It may be seen that a set of solutions up to the 20 kJ mol^{-1} potential energy contour satisfies the distance constraints. This holds for both the Abe-Man and Gal-Man glycosidic linkages, whether the contour is calculated without (Figure 9A,B) or with a hydrogen-bonding potential (Figure 9C,D). Between these two energy constraints, the impact of an intramolecular hydrogen-bonding term on the Abe-Man linkage is negligible, since the cluster of acceptable conformers that lie within in the 4–20 kJ mol^{-1} energy contour is identical. However, the situation is distinct for the Gal-Man, where the inclusion of a hydrogen-bonding term causes a segregation of solutions at the 4 kJ mol^{-1} level.

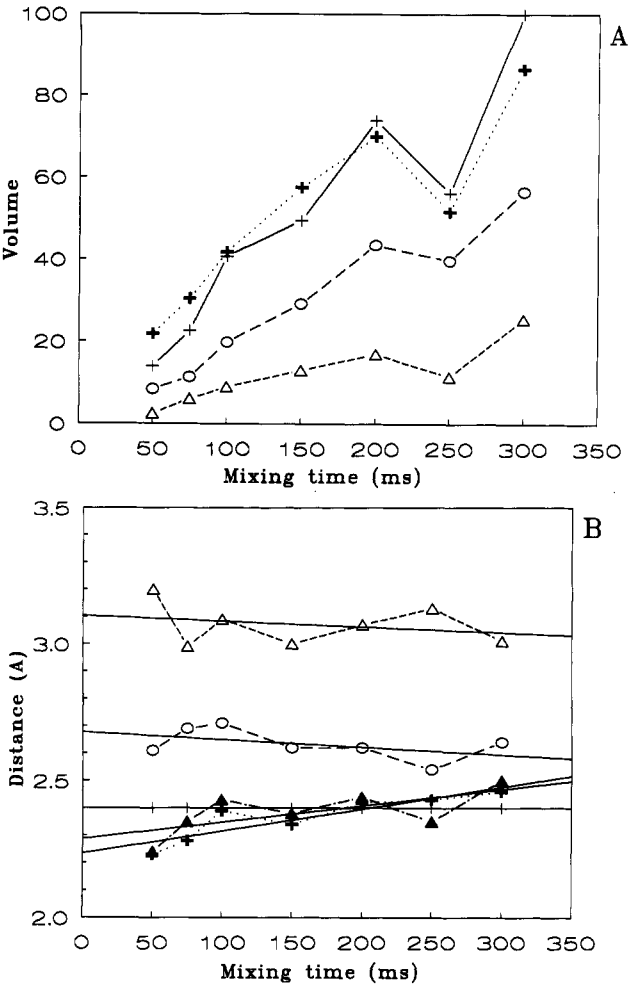

FIGURE 8: Two-dimensional TRNOE data for trisaccharide **1** with Fab. (A) NOE cross-peak volumes plotted against the mixing time for the proton pairs Gal H-1,Gal H-2 (– + –), Gal H-1,Abe H-5 (– ▲ –), Man H-1,Gal H-5 (– O –), and Gal H-1,Abe H-3 (– + –) cross-peaks. (B) Distance extrapolation from the buildup curves with Gal H-1,Gal H-2 (– + –) set at 2.4 Å, Gal H-1,AbeH-5 (– ▲ –), Man H-1,Gal H-5 (– O –), Gal H-1,Abe H-3 (– ■ –), and Abe H-3,Abe H-5 (– ▲ –).

Consequently, there are two Gal-Man conformations at ϕ,ψ = 70°,100° and 100°,100° that are consistent with the combined TRNOE and 4 kJ mol^{-1} energy constraint. When error bounds are considered, the second conformer is essentially indistinguishable from the conformation determined by crystallography, while the former is close to the global potential energy minimum. The solutions are separated by a small 8–12 kJ mol^{-1} barrier. Crystallography accurately determines interatomic distances from heavy atom coordinates, and consequently, the conversion of these into a set of torsional angles with realistic error bounds presents certain difficulties. However, within ±10° error bounds, the ϕ,ψ angles for the crystal structure solution correspond to 104°,86° for the Gal-Man linkage and 78°,95° for the Abe-Man linkage.

In order for the intramolecular hydrogen bond to form between Abe O-2 and Gal O-2, low-energy solution conformers must undergo a rotation about one or both of the glycosidic linkages. The crystal structure and TRNOE data suggest that upon binding the major ligand conformational change occurs about the Gal-Man glycosidic linkage, and in this case, the relative energy of the bound conformer compared to the global energy minima, some 14–20 kJ mol^{-1} calculated by the HSEA force field (Thøgersen *et al.*, 1981), may be attributed to the *ca.* 40° displacement of the ϕ torsional angle. In the

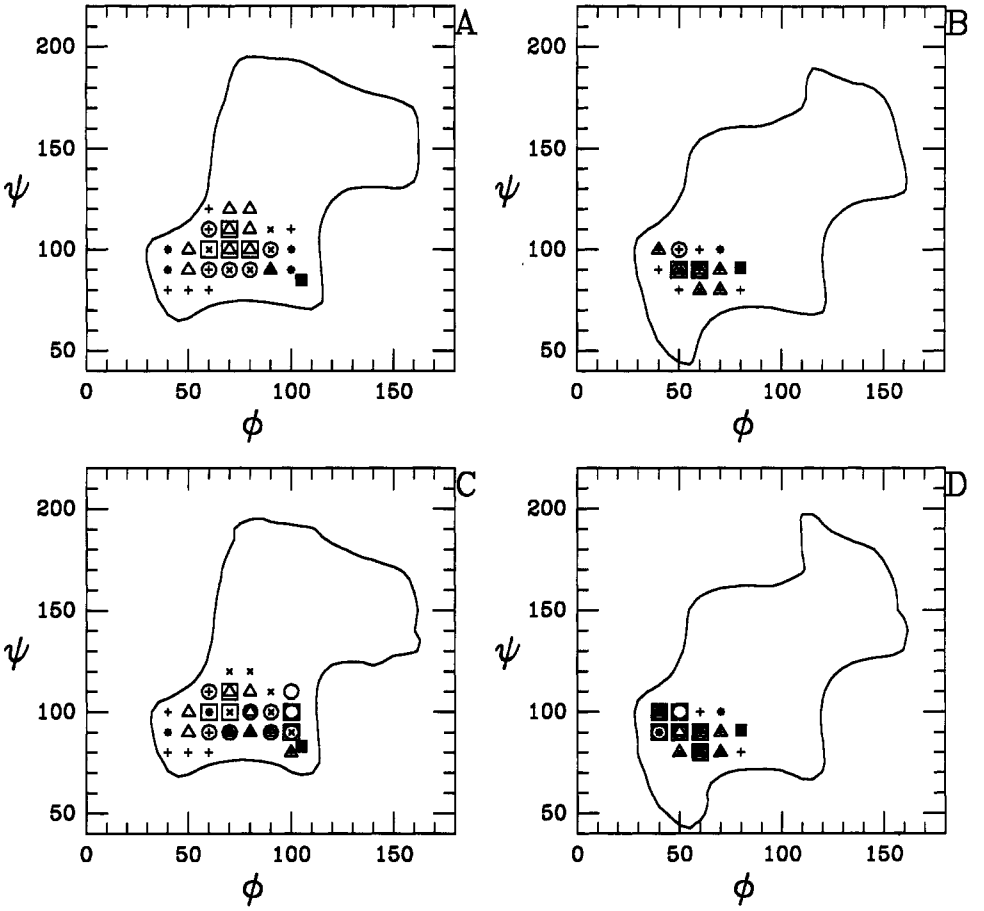

FIGURE 9: Superposition of TRNOE distance constraints and potential energy functions for the trisaccharide **1**. Two limits (Gal H-1, Abe H-3ax) between 2.2 and 2.6 Å and (Gal H-1, Abe H-5) within 2.8–3.2 Å were used to select conformers. The 40 kJ mol^{-1} energy level with respect to the unrestrained global minimum is drawn, using the HSEA potential in (A) and (B) and in (C) and (D) the HSEA potential plus an additional hydrogen-bond term. The Gal(1→2)Man linkage is shown in plots (A) and (C) and the Abe(1→3)Man linkage in plots (B) and (D). Constrained conformers within 4.2 kJ mol^{-1} intervals up to 20 kJ mol^{-1} with respect to the constrained minimum for each map are indicated by □, ○, △, ×, and +, respectively, with □ representing the lowest energy conformers. The X-ray structure is indicated by ■.

Table 6: Potential Energy Minima for Trisaccharide **1**

	torsional angles[a] (deg)		HSEA relative energy (kJ mol^{-1})	hydrogen-bond formation	gain in relative free energy due to hydrogen bond (kJ mol^{-1})
	Gal ϕ,ψ	Abe ϕ,ψ			
M1	70, 105	65, 105	0	Abe O-2···Gal O-2	−3.5
M2	80, 145	70, 125	−2	Abe O-2···Gal O-2	−1.4
M3	95, 95	60, 95	−10	Abe O-2···Gal O-2	
M4	125, 125	135, 145	−17	Abe O-2···Man O-4	−3.5
M5	80, 120	100, 100	−13	Abe O-2···Man O-4	−2.0

[a] ϕ = O-5–C-1–O-1–C′$_x$, ψ = C-1–O-1–C′$_x$–C′$_{x+1}$.

preceding manuscript, $\Delta(\Delta G)$ values for modified derivatives of **1** with and without the galactose residue fell within the 2–5 kJ mol^{-1} range. This modest energy difference suggests that the energy penalty for binding a disfavored Gal conformer may be offset by favorable protein–saccharide and saccharide–saccharide interactions.

CONCLUSIONS

The bound conformation observed for trisaccharide **1** by crystallography shows an intramolecular bond between Abe O-2 and Gal O-2, but attempts to detect this hydrogen bond in aqueous solution were unsuccessful. Although this conformation is probably sampled by the internal motions about glycosidic linkages, there is no evidence to suggest that this hydrogen bond favors or stabilizes a preferred solution conformation.

Transferred NOE measurements show that the problems of interconverting oligosaccharide conformations detected by NOE difference spectroscopy for free ligand are considerably simplified when oligosaccharide is bound by Fab. By extrapolating proton internuclear distances to zero mixing time, it was shown that only two bound conformations are consistent with low-energy trisaccharide conformations. One of these corresponds to the crystal structure observed in the trisaccharide–Fab complex. Long-range NOEs between two pyranose residues that are not covalently linked provide a very sensitive probe of the oligosaccharide conformation since small changes in the ϕ,ψ angles lead to large changes in interproton distances, *e.g.*, Gal H-1 to Abe H-3ax or Abe H-5 (Figures 6 and 7), and the change observed for these NOEs as the free ligand is bound suggests that the antibody imposes an induced fit on the trisaccharide epitope.

The change in torsional angle upon binding lies within the range of conformers sampled in solution and in general terms validates the simple assumptions used to interpret functional group replacements in the preceding paper (Bundle *et al.*, 1994).

REFERENCES

Allerhand, A., Doddrell, D., & Komorski, R. (1971) *J. Chem. Phys. 55*, 189–198.

Baleja, J. D., Moult, J., & Sykes, B. D. (1990) *J. Magn. Reson. 87*, 375–384.

Bevilacqua, V. L., Thomson, D. S., & Prestegard, J. H. (1990) *Biochemistry 29*, 5529–5537.

Bevilacqua, V. L., Kim, Y., & Prestegard, J. H. (1992) *Biochemistry 31*, 9339–9349.
Bock, K., Meldal, M., Bundle, D. R., Iversen, T., Garegg, P. J., Norberg, T., Lindberg, A. A., & Svenson, S. B. (1984a) *Carbohydr. Res. 130*, 23–34.
Bock, K., Meldal, M., Bundle, D. R., Iversen, T., Pinto, B. M., Garegg, P. J., Kvanstrom, I., & Norberg, T. (1984) *Carbohydr. Res. 130*, 35–53.
Bock, K., Frejd, T., Kihlberg, J., & Magnusson, G. (1988) *Carbohydr. Res. 176*, 253–270.
Bock, K., Lönn, H., & Peters, T. (1990) *Carbohydr. Res. 198*, 375–380.
Brooks, B. R., Bruccoleri, R. E., Olafson, B. D., States, D. J., Swaminathan, S., & Karplus, M. (1983) *J. Comput. Chem. 4*, 187–217.
Bruderer, U., Peyton, D. H., Barbar, E., Fellman, J. H., & Rittenberg, M. B. (1992) *Biochemistry 31*, 584–589.
Bundle, D. R., & Eichler, E. (1994) *Bioorg. Med. Chem.* (in press).
Bundle, D. R., Eichler, E., Gidney, M. A. J., Meldal, M., Ragauskas, A., Sigurskjold, B. W., Sinnott, B., Watson, D. C., Yaguchi, M., & Young, N. M. (1994) *Biochemistry* (preceding paper in this issue).
Cagas, P., & Bush, C. A. (1990) *Biopolymers 30*, 1123–1138.
Christofides, J. C., Davies, D. B., Martin, J. A., & Rathbone, E. B. (1986) *J. Am. Chem. Soc. 108*, 5738–5743.
Clore, G. M., & Gronenborn, A. M. (1982) *J. Magn. Reson. 48*, 402–417.
Clore, G. M., & Gronenborn, A. M. (1983) *J. Magn. Reson. 53*, 423–442.
Colman, P. M. (1988) *Adv. Immunol. 43*, 99–132.
Cumming, D. A., & Carver, J. P. (1987) *Biochemistry 26*, 6664–6676.
Cygler, M., Rose, D. R., & Bundle, D. R. (1991) *Science 253*, 442–445.
Davies, D. R., Padlan, E. A., & Sheriff, S. (1990) *Annu. Rev. Biochem. 59*, 439–73.
Freeman, R., & Hill, H. D. W. (1970) *J. Chem. Phys. 53*, 4103–4105.
Glaudemans, C. P. J., Lerner, L., Davies, G. D., Jr., Kovac, P., Venable, R., & Bax, A. (1990) *Biochemistry 29*, 10906–10911.
Ha, S. N., Giammona, A., Field, M., & Brady, J. W. (1988) *Carbohydr. Res. 180*, 207–221.
Herman, J. N., He, X.-M., Mason, L., Voss, E. W., Jr., & Edmundson, A. B. (1989) *Proteins 5*, 271–280.
Homans, S. W. (1990) *Biochemistry 29*, 9110–9118.
Hricovini, M., Shah, R. N., & Carver, J. P. (1992) *Biochemistry 31*, 10018–10023.
Jorgensen, W. L. (1991) *Science 254*, 954–955.
Kabat, E. A. (1996) *J. Immunol. 97*, 1–11.
Lavoie, T. B., Drohan, W. N., & Smith-Gill, S. J. (1992) *J. Immunol. 148*, 503–513.
Lemieux, R. U., & Bock, K. (1982) *Carbohydr. Res. 100*, 63–74.
Lemieux, R. U., & Bock, K. (1984) *Jpn. J. Antibiot. 32*, 163–167.
Lüderitz, O., Straub, A. M., & Westphal, O. (1966) *Bacteriol. Rev. 30*, 192–255.
Meyer, B. (1990) in *Topics in Current Chemistry; Carbohydrate Chemistry* (Theim, J., Ed.) Vol. 154, pp 141–208, Springer, Berlin.
Peters, T., Brisson, J.-R., & Bundle, D. R. (1990) *Can. J. Chem. 68*, 979–988.
Poppe, L., & van Halbeek, H. (1991) *J. Am. Chem. Soc. 113*, 363–365.
Poppe, L., & van Halbeek, H. (1992) *J. Am. Chem. Soc. 114*, 1092–1094.
Poppe, L., Stuike-Prill, R., Meyer, B., & van Halbeek, H. (1992) *J. Biomol. NMR 2*, 109–136.
Rini, J. M., Schulze-Gahmen, U., & Wilson, I. A. (1992) *Science 255*, 959–965.
Rose, D. R., Cygler, M., To, R. J., Przybylska, M., Sinnott, B., & Bundle, D. R. (1990) *J. Mol. Biol. 215*, 489–492.
Scherf, T., Hiller, R., Naider, F., Levitt, M., & Anglister, J. (1992) *Biochemistry 31*, 6884–6897.
Sklenar, V., & Bax, A. (1987) *J. Magn. Reson. 75*, 378–383.
Sigurskjold, B. W., Altman, E., & Bundle, D. R. (1991) *Eur. J. Biochem. 197*, 239–246.
Stanfield, R. L., Fieser, T. M., Lerner, R. A., & Wilson, I. A. (1990) *Science 248*, 712–719.
Stevens, S. Y., Swanson, P. C., Voss, E. W., Jr., & Glick, G. D. (1993) *J. Am. Chem. Soc. 115*, 1586–1588.
Thøgersen, H., Lemieux, R. U., Bock, K., & Meyer, B. (1981) *Can. J. Chem. 60*, 44–57.
Vyas, M. N., Vyas, N. K., Meikle, P. J., Sinnott, B., Pinto, B. M., Bundle, D. R., & Quiocho, F. A. (1993) *J. Mol. Biol. 231*, 133–136.
Wiberg, K. B., & Murcko, M. A. J. (1989) *J. Am. Chem. Soc. 111*, 4821–4828.